Asian Journal of Information Technology 15 (13): 2167-2176, 2016
ISSN: 1682-3915

Severity Analysis of Cervical Cancer in PAP Smear Images Using Textures Features and Hybrid RBF Kernel Based SVM

[1]G. Hariharan, [2]A. Jayachandran, [3]G. Jiji, [4]M.Rajaram and [3]T. Ajith Bosco Raj
[1]Department of CSE, PSN Engineering College, Tirunelveli, India
[2]Department of CSE, PSN College of Engineering and Technology, Tirunelveli, India
[3]Department of ECE, PSN College of Engineering and Technology, Tirunelveli, India
[4]Department of EEE, College of Engineering Guindy, Anna University Chennai,
600 025 Chennai, India

Abstract: Classification of medical imagery is a difficult and challenging process due to the intricacy of the images and lack of models of the anatomy that completely captures the possible deformations in each structure. Cervical cancer is one of the major causes of death among other types of the cancers in women world wide. Proper and timely diagnosis can prevent the life to some extent. Therefore we have proposed an automated reliable system for the diagnosis of the cervical cancer using texture features and machine learning algorithm in PAP smear images, it is very beneficial to prevent cancer also increases the reliability of the diagnosis. In this research study, we have developed, multi class cervical cancer severity analysis system based on hybrid texture features and hybrid RBF kernel based support vector machine using PAP smear images. Two major contribution of the proposed system is feature extraction and feature classification. In feature extraction, multiple features are extracted using texture features and Gabor filter based orientation image. This system classifies the PAP smear cells into anyone of four different types of classes using RBF-SVM. The performance of the proposed algorithm is tested and compared to other algorithms on public image database of Herlev University Hospital, Denmark with 452 PAP smear images. The overall classification accuracy of the proposed hybrid RBF-SVM is 96.8% but the existing methods RBF and SVM produce 91.32 and 94.32%, respectively.

Key words: RBF-SVM, PAP smear images, machine, cervical cancer, extraction

INTRODUCTION

Cervical cancer is one of the crucial reasons of cancer death in females universal. The PAP smear is the extreme active screening test used to perceive the cervical pre-cancerous and cancerous variations in a experimental of cervical cells based on the shape variations of the nuclei and cytoplasm (Kiviat, 1996; Kurman *et al*., 1994). PAP test has severely altered the prognosis of women with cervical cancer as it has exhibited its ability to detect 95% of the cancers of the vaginal neck . Cervical cancer can be prevented if it is perceived and treated early (Marinakis *et al*., 2008). PAP smear test is a physical screening process used to identify cervical cancer or precancerous changes in an uterine cervix by grading cervical cells based on color, shape and texture properties of their nuclei and cytoplasms. A computer-assisted screening structure for PAP smear tests will be exact helpful to prevent cervical cancer if it increases the reliability of the diagnosis (Pradhan and Sinha, 2010). PAP anicolaon (PAP) Smear Screening Test is the most common form of diagnosis for detecting cervical cancer in its early stages. Cervical cancer is a disease that occurs when cells in the cervix area instigate to produce out of controller and attack nearby tissues or feast throughout the body. Cancer or tumor can be divided into two groups, i.e., benign and malignant. Benign, that does not attack and abolish the tissue in which it originates or spread to aloof sites in the body (non-cancerous tumor) while malignant that attacks and abolishes the tissue in which it invents and can feast to other sites in the body via blood-stream and lymphatic system (cancerous tumor) (Mustafa *et al*., 2004; Khotanlou *et al*., 2009; Mishra, 2010).

Medical image processing syatem has lead to an increasing important and evolving role for image processing and Computer-Aided Diagnosis (CAD) systems in numerous clinical applications. Cervical cancer is the second most common cancer affecting women worldwide and the leading cause of cancer mortality in developing countries. It can be cured in almost all patients, if detected early and treated adequately. An

Corresponding Author: G. Hariharan, Department of CSE, PSN Engineering College, Tirunelveli, India

automated image analysis system of uterine cervical images analyzes and extracts diagnostic features in cervical images and can assist the physician with a suggested clinical diagnosis. Such a system could be integrated with a medical screening device to allow screening for cervical cancer by non-medical personnel (Shen *et al*., 2005; Lin *et al*.,1996).

Image segmentation is a serious component of image recognition and analysis system. It plays a significant role in biomedical imaging applications such as the inventory of tissue volumes diagnosis, localization of pathology analysis of anatomical structure, treatment plannin, partial volume upgrading of practical imaging data and computer integrated surgery (Peng *et al*., 2010; Yang *et al*., 2008). Medical Image segmentation is to partition the image into a set of regions that are visually obvious and consistent with respect to some properties such as gray level, texture or color. On the other hand, feature extraction is one of the most important methods for capturing visual content of an image. To facilitate decision making such as pattern classification, feature extraction is used as the process to represent the raw image in its reduced form. This approach combines the intensity, texture, shape based features and classifies the tumor as white matter, gray matter, CSF, abnormal and normal area. The various methods such as Multi Texton Histogram (MTH), Principal Component Analysis (PCA) Texton co-occurrence matrix and Linear Discriminant Analysis (LDA) are used for reducing the number of features (Mustafa *et al*., 2014). The MTH is a feature extractor and a descriptor to retrieve the content image which integrates the advantages of representing the attribute of the co-occurrence matrix using histograms (Jayachandran and Dhanasekaran, 2013). This descriptor analyzes the spatial correlation between neighboring color and edge orientation based on four special texton types (Julesz, 1981).

The feature extraction plays an important role in Cervical cancer classification process, whose effectiveness depends upon the method adopted for extracting features from given images. The visual content descriptors are either global or local. A global descriptor represents the visual features of the whole image; whereas a local descriptor represents the visual features of regions or objects to describe the image. These are arranged as multidimensional feature vectors and construct the feature database. For similarity distance measurement many methods have been developed like Euclidean distance (L2), L1 distance, etc. Selection of feature descriptors and similarity distance measures affect performances of an cervical cancer classification system significantly (Mukhopadhyay and Chanda, 2003). In this research article, we have developed a cervical cancer detection system that is able to detect and categorized cervical cells into normal and cancerous cells based on texture features and machine learning method.

MATERIALS AND METHODS

Proposed cervical cancer classification system: Classification of medical imagery is a knotty and challenging process due to the intricacy of the images and lack of models of the anatomy that completely captures the possible deformations in each structure. Cervical cancer is the supreme common malignancy in women in the emerging countries. Cervical cancer grows over a protracted period covering two to three decades. Cervical cancer is the most common form of cancer in women under 35 years of age and the second most commonly occurring cancer in women of all ages, worldwide (Mustafa *et al*., 2004). In our proposed, cervical cancer classification systems consists of preprocessing, segmentation, feature extraction and feature classification. In feature extraction, multiple features are used to determine the relevance of normal and abnormal images. In this scenario, it is essential to minimize all the features distances that are determined between the cancer image and the non cancerous images. To perform the classification stage efficiently, an effective classification algorithm is required. In this research, we exploit the proposed hybrid algorithm in the classification stage to ensure the classification performance. Our proposed method consists of three phases namely, cervical cell nucleus detection, feature extraction and classification. In this studyr, cervical cell nucleus detection is done using pre-processing and segmentation process. In pre-processing, anisotropic filter is applied to remove the noise and enhance the image for the cell Nucleus detection process.

Cervical cell nucleus detection: It is the crucial stage in the entire process. Pre-processing and segmentation process are the steps to the tumor region identification stage. Preprocessing on the input image is extremely essential, so that the image gets altered to be related to the further processing. In this study, experimental images cannot be given directly the segmentation process. The input image is passed through an anisotropic filter which diminishes the noise and enhances the image quality. Anisotropic filter is used for reducing image noise without removing significant parts of the image content, particularly the edges, lines or other details that are important for the interpretation of the image (Demirkaya, 2009). The proposed cervical cell nucleus detection process consists of three stages such as:

- Image binarization using thresholding
- Sharpening the region using morphological operations
- Nucleus region identification

Original image is covert into a binary image by thresholding: Initially, the input image is transformed into a binary image. An image of up to 256 gray levels is translated to a black and white image using the threshold value. The gray level value of every pixel in the improved image is considered at this stage. All the pixels with values above the threshold are set as white and the remaining pixels are set as black in the image during the binarization process. In this study, the threshold value is selected based on the contrast of the image.

$$\text{Binarized image, } B_{Binary}(k,y) = \begin{cases} 0, \text{if } B_{grey}(k,y) \le \text{Threshold} \\ 1, \quad \text{Otherwise} \end{cases} \quad (1)$$

Sharpening the region using morphological operation: After transforming into binary images, the morphological process is applied for sharpening the regions and filling the gaps. The main processes of the morphological operations are opening, closing, erosion and dilation. In this study, erosion operation is applied for removing the hurdle, noise and enhances the image.

Erosion: In the erosion operation on an image F having labels 0 and 1 with structuring element Y, the value of pixel i in F is changed from 1-0, if the result of convolving Y with F, centered at i is below some predefined value. We have set this value to be the area of Y which is principally the number of pixels that are 1 in the structuring element itself. The structuring element also known as the erosion kernel, finds out the details of how particular erosion thins boundaries:

$$IE = \text{imerode}(F, Y)$$

Nucleus area identification: After the morphological operation, the nucleus regions are identified via a regionprops algorithm. The regions of the nucleus are marked out based on their area properties. The regionprops algorithm measures the properties of image regions. Using the actual number of pixels in the region, the nucleus region's area is segmented. This value is slightly different from the value returned by bwarea which weights diverse patterns of pixels in a different way. The regionprops calculates the area by measuring the distance between each neighboring pair of pixels around the border of the region. After the segmentation process is completed, we get the segmented nucleus from its surrounding cytoplasm. But the results were somewhat light portioning of the nucleus. For this reason, researchers have gone for the enhancement process to enhance or increase the contrast of the nucleus.

Feature extraction process: The process of extracting the features of the high contrast image sequence in a temporal frame with gray scale reference information for text block detection in both horizontal and vertical edge scanning of adjacent text block in a multi-resolution fashion are considered as feature extraction. It extracts information grounded on maximum gradient difference. The purpose of feature extraction is to reduce the original data set by measuring certain properties or features, that distinguish one input pattern from another pattern. The extracted feature is expected to provide the characteristics of the input type to the classifier by considering the description of the relevant properties of the image into a feature space. The proposed method feature extraction process consists of five steps such as:

- Computation of Feature Vector F(V1) using LoG
- Computation of Feature Vector F(V2) using GLCM
- Computation of Feature Vector F(V3) using DGTF
- Computation of Feature Vector F(V4 using RICGF
- Concatenation of four feature vector

Laplacian of Gaussian (LoG): LoG filters at Gaussian widths of 0.25, 0.50, 1 and 2 are considered. These values are convoluted with the input image. Sixteen features are retrieved by calculating mean, standard deviation, skewness, autocorrelation, busyness, coarseness and kurtosis for the LoG filter output in the SROI region.

Mean: The mean (m) is defined as the sum of the intensity values of pixels divided by the number of pixels in the SROI of an image.

Standard deviation: It shows how much variation or exists from the expected value i.e., the mean. The data points tend to be very close to the mean results low standard deviation and the data points are spread out over a large range of values results high standard deviation.

Skewness: It is a measure of the asymmetry of the data around the sample mean. If the value is negative, the data are spread out more to the left of meaner than to the right. If the value is positive, the data are spread out more to the right. The sickness of the normal distribution (or any perfectly symmetric distribution) is zero. The skewness of a distribution is defined as:

$$Y=E\,(x-\mu)^3/\sigma^3$$

Where:
μ = The mean of x
σ = The standard deviation of x
E(t) = Represents the expected value of the quantity t

Autocorrelation: It is used to evaluate the quantity of promptness as well as the excellence of the texture present in the image, denoted as $f(\delta_i, \delta_j)$. For a n×m image is defined as follows:

$$f(\delta_i,\delta_j)=\frac{1}{(n-\delta_i)(m-\delta_j)}\sum_{i=1}^{n-\delta_i}\sum_{j=0}^{m-\delta_j} I(i,j)I(i+\delta_i,j+\delta_j)$$

Here, $1\le\delta_i\le n$ and $1\le\delta_j\le m$. The δ_i and δ_j represent a shift on rows and columns, respectively.

Kurtosis: The forth central moment gives kurtosis. It gives the measure of closeness of an intensity distribution to the normal Gaussian shape:

$$\text{Kurtosis}=\frac{1}{N}\frac{\sum_i\sum_j\left(I(i,j)-m\right)^4}{\text{Std}^4}$$

Coarseness: The Coarseness is calculated based on the Shape. This value is not equal to zero then the segmented area has been affected by the tumor, otherwise the tumor does not affect the segmented area. It is the average number of maxima in the autocorrelated images and original images. The Coarseness (Cs) is calculated as follows:

$$C_S=\frac{1}{0.5\left(\sum_{i=1}^{n}\sum_{j=1}^{m}\text{Max}(i,j)/n+\sum_{i=1}^{n}\sum_{j=1}^{m}\text{Max}(i,j)/m\right)}$$

Busyness: It is calculated based on connectivity, how much the pixels are connected is calculated that is above 5 then the segmented area has a tumor. The business' value is below 5 the segmented area does not have a tumor. Thebusyness value is depending on Coarseness. If the value of coarseness is high, the It is related to coarseness in the reverse order that is when the business is low:

$$B_S=1-C_S^{\frac{1}{\alpha}}$$

Computation of Feature Vector F(V2) using GLCM: Gray-level-based features: features based on the differences between the gray-level in the candidate pixel and a statistical value representative of its surroundings. It contains the second-order statistical information of neighboring pixels of an image. It is estimated of a joint Probability Density Function (PDF) of gray level pairs in an image (Cobzas *et al*., 2007). It can be expressed in the following equation:

$$P_\mu(i,j)\,(i,j=0,1,2,...,N-1)$$

Where:
i, j = Indicate the gray level of two pixels
N = The gray image dimensions
μ = The position relation of two pixels

Different values of μ decides the distance and direction of two pixels. Normally Distance (D) is 1, 2 and Direction (θ) is 0°, 45°, 90°, 135° are used for calculation (Daugman, 1988). Texture features can be extracted from gray level images using GLCM matrix . In our proposed method, five texture features energy, contrast, correlation, entropy and homogeneity are experiments. These features are extracted from the segmented MR images and analyzed using various directions and distances. Energy expresses the repetition of pixel pairs of an image:

$$k1=\sum_{i=0}^{N-1}\sum_{j=0}^{k-1}P_\mu^2(i,j)$$

Local variations present in the image is measured by Contrast. If the contrast value is high means the image has large variations:

$$k2=\sum_{t=0}^{N-1}t^2\left\{\sum_{i=0}^{N-1}\sum_{i=0}^{N-1}P_\mu(i,j)\right\}$$

Correlation is a measure linear dependency of gray level values in co-occurrence matrices. It is a two dimensional frequency histogram in which individual pixel pairs are assigned to each other on the basis of a specific, predefined displacement vector:

$$k3=\sum_{i=0}^{k-1}\sum_{j=0}^{k-1}\frac{(i,j)P(i,j)-\mu_1\mu_2}{\sigma_1^2\sigma_2^2}$$

where, μ_1, μ_2, σ_1, σ_2 are mean and standard deviation values accumulated in the x and y directions respectively. Entropy is a measure of non-uniformity in the image based on the probability of Co-occurrence values, it also indicates the complexity of the image:

$$k4=-\sum_{i=0}^{k-1}\sum_{j=0}^{k-1}P_\mu(i,j)\log\left(P_\mu(i,j)\right)$$

Homogeneity is inversely proportional to contrast at constant energy whereas it is inversely proportional to energy:

Table 1: Summary of intensity and texture features

Feature Category	Features	No. of features
LoG	Four statistical parameters for the LoG filter output in the SROI region are retrieved at $\sigma = 0.25, 0.50, 1$ and 2 thereby contributing 16 features in the feature pool. These parameters are: mean intensity, standard deviation, skewness, kurtosis	16 features
GLCM	Following GLCM features at 0°, 45°, 90° and 135° are calculated: contrast, homogeneity, correlation, energy	4*4 = 16 features
DGTF	DGTFs are calculated at λ for $2\sqrt{2}$, 4, $4\sqrt{2}$, 8, $8\sqrt{2}$) and θ for 0°, 22.5°, 45°, 67.5° and 90° are varied. Four statistical parameters are calculated for each filter output in the marked SROI and are taken as 100 features in the feature bank. These parameters are: mean intensity, standard deviation, Skewness, Kurtosis	25* 4 = 100 features
RICGFs	RICGFs are calculated at $\lambda = 2\sqrt{2}$, 4, $4\sqrt{2}$, 8, $8\sqrt{2}$) and two values of ψ, i.e., 0° and 90° four statistical parameters for each filter output in the marked SROI and are taken as 40 features in the feature bank. These features are: mean intensity, standard deviation, skewness, kurtosis	10* 4 = 40 features

$$k5 = \sum_{i=0}^{k-1}\sum_{j=0}^{k-1}\frac{p_{\mu}(i,j)}{1+(i,j)^2}, i \neq j$$

Directional Gabor Texture Features (DGTF): Directional Gabor's are used as they measure the heterogeneity in the SROI. Gabor filter is a Gaussian kernel function modulated by a sinusoidal plane wave. There fore, it gives directional texture features at a specified Gaussian scale. Gabor kernel is defined as:

$$g(x,y,\lambda,\theta,\psi,\sigma,\gamma) = \exp\left(-\frac{x'^2+\gamma^2y'^2}{2\sigma^2}\right)\times \cos\left(2\pi\frac{x'}{\lambda}+\psi\right)$$

$$\text{Where, } x' = x\cos\theta + y\sin\theta,$$

$$y' = -x\sin\theta + y\cos\theta'$$

Where:

- λ = Represents the wavelength of the sinusoidal factor
- θ = Represents the orientation of the normal to the parallel stripes of a Gabor function
- ψ = The phase offset
- σ = The width of the Gaussian
- γ = The spatial aspect ratio and specifies the ellipticity of the support of the Gabor function

The intensity and texture features summary is given in Table 1.

Rotation Invariant Circular Gabor Features (RICGF): Gabor filter is a Gaussian kernel function modulated by a radially sinusoidal surface wave; therefore, it gives rotational invariant texture features which are given by:

$$g(x,y,\lambda,\theta,\psi,\sigma,\gamma) = \exp\left(-\frac{D(x,y)^2}{2\sigma^2}\right)\times\cos\left(2\pi\frac{D(x,y)}{\lambda}+\psi\right)$$

$$\text{Where, } D(x,y) = \sqrt{(x-\bar{x})^2+(y-\bar{y})^2}$$

Where:

- λ = Represents the wavelength of the sinusoidal factor
- θ = Represents the orientation of the normal to the parallel stripes of a Gabor function
- ψ = The phase offset
- σ = The width of the Gaussian
- γ = The spatial aspect ratio and specifies the ellipticity of the support of the Gabor function

Hybrid RBF kernel-SVM classifier: The diagnostic models, hybrid kernel based SVM has been developed for improving the classification process. The extracted textures features are used for the separation of two classes such as cancer and non-cancerous. Since the texture feature follows the non-linearity, non-linear SVM is needed to do the separation of hyperplane. To do non-linear task, kernel functions are introduced in SVM classification. Multiple kernels are combined to develop a new hybrid kernel that will improve the classification task of separating the training data. By introducing the hybrid kernel, SVMs gain flexibility in the choice of the form of the threshold which need not be linear and even not to have the same functional form for all data, since its function is non-parametric and operates locally.

In most of the cases, an object is assigned to one of the several categories based on some of its characteristics in the real life situation. For instance, based on the outcome of several medical tests, it is mandatory to say whether the patient has a particular disease or not. In computer science such situations are explained as classification issue. There are two phases in the support vector machine namely, Training phase and Testing phase.

Training phase: The output from the improved multi-texton is given as input to the training phase. The input function gives the set of values which are non separable. All the possible separations of the pointset can

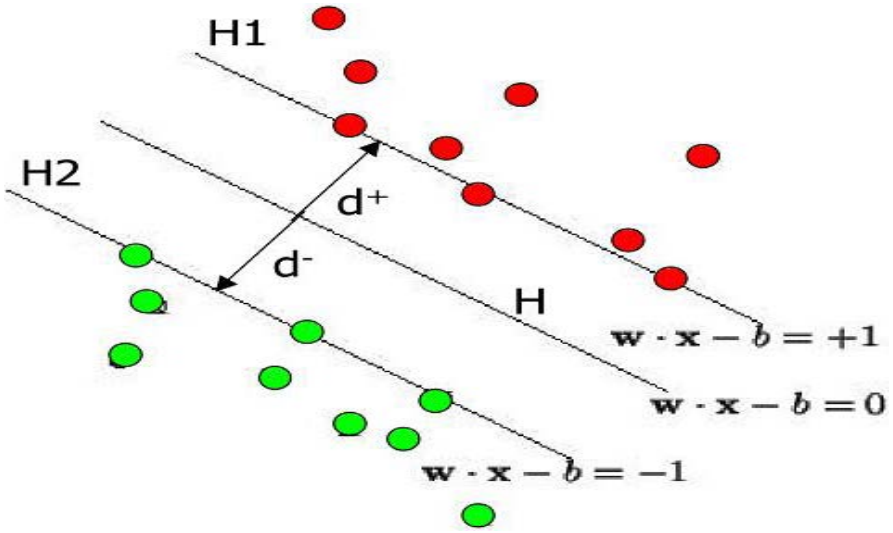

Fig. 1: Sample representation of separating optimal hyper plane

be achieved by a hyperplane. For that, a set of data drawn from an unknown distribution $((x_1,y_1),...,(x_l,y_l), x_l \in R^n, y_1 \in \{-1,1\}$ and also a set of decision functions or hypothesis space $f_\lambda:\lambda \epsilon \Lambda$ are given where Λ (an index set) is a set of abstract parameters, not necessarily vectors. f_λ: $R^n \rightarrow \{-1,+1\}$ is also called a hypothesis. The set of functions f_λ could be a set of Radial Basis Functions or a multi-layer neural network. All the possible separations of the point set can be achieved by a hyperplane. In the Lagrange optimization formulation we can find the optimal separating hyperplane normal vector. A kernel is any function K: $R^n \times R^n \rightarrow R$. This corresponds to a dot product for some feature mapping:

$$K(X_1, X_2) = \phi(X_1)\phi(X_2) \text{ For some } \phi \quad (2)$$

The kernel function can directly compute the dot product in the higher dimensional space. Introduce kernel-based Lagrange multipliers $\alpha_i \geq 0 \forall_i$:

$$L_p = \sum_{i=1}^{n} \alpha_i - \frac{1}{2} \sum_{i=1}^{n} \sum_{i=1}^{n} \alpha_i \alpha_j y_i y_j K(x_i . x_j) \quad (3)$$

Minimize L_p with respect to w, b and maximize with respect to α_i. In a convex quadratic programming problem, the plane is a nonlinear combination of the training vectors:

$$w = \sum_{i=1}^{n} \alpha_i y_i K(x_i) \quad (4)$$

Thus, the hyperplane is separated into two clusters. The sample representation of this process is shown in Fig. 1. The point on the planes H_1 and H_2 is the support vectors. H_1 and H_2 are the planes:

- d^+ = The shortest distance to the closest positive point
- d^- = The shortest distance to the closest negative point
- $d^+ + d$ = Represents the margin of a separating hyper plane

Testing phase: The output from the improved multi-texon is given as an input MRI image to the testing phase and the output MRI image shows whether a tumor is present or not. The class of an input data x is then determined in Eq. 5:

$$\text{class}(x) = \text{sign}(\varphi(x).w - b) = \text{sign}\left(\sum y_i \lambda_i \varphi(x_i).\varphi(x) - b\right) \quad (5)$$

We have analyzed the kernel equation from the existing research (Chen *et al*., 2011; Martin, 2003) and used them in the proposed research namely, RBF and quadratic function.

Radial basis function: The support vector will be the centre of the RBF and σ will determine the area of influence. This support vector has the data space:

$$K(x_i, x_j) = \exp\left(-\frac{\|x_i - x_j\|^2}{2\sigma^2}\right)$$

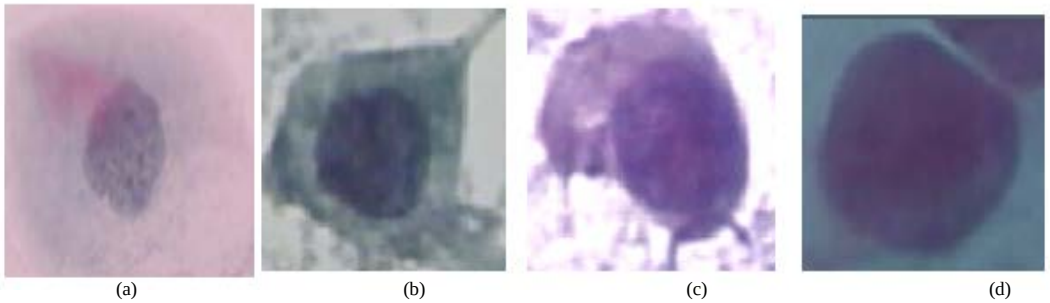

(a) (b) (c) (d)

Fig. 2: Some of the cells found in cervix: A-C) mild, moderate and severe dysplasia, (D) Carcinoma *in situ*

Quadratic kernel function: Polynomial kernels are of the form:

$$K(\vec{x},\vec{z}) = \left(1+\vec{x}^{T}\vec{z}\right)^{d}$$

where, d = 1, a linear kernel and d = 2, a quadratic kernel are commonly used. Let k_1(RBF) and k_2 (Quadratic) be kernels over $\Xi\times\Xi$, $\Xi\subseteq R^p$ and K_3 be a kernel over $R^p\times R^p$. Let function φ: $\Xi\rightarrow R^p$. The four kernel based formulations are represented by:

$$k(x,y) = k_1(x,y) + k_2(x,y) \text{is a kernal} \quad (6)$$

$$k(x,y) = k_1(x,y)k_2(x,y) \text{is a kernal} \quad (7)$$

Substitute the two Eq. 6 and 7 in Lagrange multiplier Eq. 8 and get the proposed hybrid kernel. It is exposed in Eq. 9:

$$L_p = \sum_{i=1}^{n}\alpha_i - \frac{1}{2}\sum_{i=1}^{n}\sum_{i=1}^{n}\alpha_i\alpha_i y_i y_i\left(k_1\left(x_i.x_j\right) + k_2\left(x_i.x_j\right)\right) \quad (8)$$

$$L_p = \sum_{i=1}^{n}\alpha_i - \frac{1}{2}\sum_{i=1}^{n}\sum_{i=1}^{n}\alpha_i\alpha_j y_i y_j k_1\left(x_i.x_j\right)k_2\left(x_i.x_j\right) \quad (9)$$

Substitute the four theorems in Quadratic function Eq. 10 and get:

$$w = \sum_{i=1}^{n}\alpha_i y_i\left(K_1(x_i) + k_2(y_i)\right) \quad (10)$$

$$w = \sum_{i=1}^{n}\alpha_i y_i \alpha K_1(x_i)k_2(y_i) \quad (11)$$

RESULTS AND DISCUSSION

Data set and parameter description: The experimental PAP smear images are acquired through a powerful micro scope by the skilled cyto-technicians. All images were captured with a resolution of 0.201 μm/pixel from the open bench mark database of cervical cancer, Herlev University Hospital, Denmark. The images were prepared and analyzed by the staff at the hospital using a commercial software package CHAMP[2] for segmenting the images. The cells were selected, not to collect a natural distribution but to make a good collection of the important classes such as mild dysplasia, moderate dysplasia, Severe dysplasia and carcinoma in situ. The sample PAP smear experimental images of various classes is shown in Fig. 2. The data set contains 452 images with the following abnormal class distribution:

- Mild dysplasia, 113 images
- Moderate dysplasia, 105 images
- Severe dysplasia, 110 images
- Carcinoma in situ, 114 images

This study describes the experimental results of the proposed classification method using PAP smear images with different types of cervical cancer. In the proposed method, the experimental image data set is divided into two sets such as training set and testing set. The classifiers are trained with the training images and the classification accuracy is calculated only with the testing images. In the testing phase, the testing dataset is given to the proposed technique to find the cancers type in smear images and the obtained results are evaluated through evaluation metrics namely, sensitivity, specificity and accuracy, it is given by:

$$\text{Sensitivity} = TP/(TP+FN)$$

$$\text{Specificity} = TN/(TN+FP)$$

$$\text{Accuracy} = (TN+TP)/(TN+TP+FN+FP)$$

Where:
TP = Corresponds to True Positive
TN = Corresponds to True Negative
FP = Corresponds to False Positive
FN = Corresponds to False Negative

These parameters for a specific category, say, Mild dysplasia are as follows: TP is True Positive (an image of 'Mild dysplasia' type is categorized correctly to the same type), TN = True Negative (an image of 'Non-mild dysplasia' type is categorized correctly as 'Non-mild dysplasia' type), FP = False Positive (an image of 'Non-mild dysplasia' type is categorized wrongly as 'Mild dysplasia' type) and FN is False Negative (an image of 'Mild dysplasia' type is categorized wrongly as 'Non-mild dysplasia' type). 'Non-mild dysplasia' actually corresponds to any of the three categories other than 'Mild dysplasia'. Thus, 'TP and TN' corresponds to the correctly classier images and 'FP and FN' corresponds to the misclassified images (Table 2).

The same feature sets are determined for all the categories by replacing 'Mild dysplasia' in the above de?nitions with other cancer categories. Thus, different parameter values are obtained for each class and also for the different classifiers. These parameters are estimated from the confusion matrix which provides the details about the false and successful classification of images from all categories for each classifiers. The confusion matrix of the proposed method is illustrated in Table 3.

Table 3 shown the row-wise elements correspond to the four categories and the column-wise elements correspond to the target class associated with that abnormal category. Hence, the number of images correctly classified (TP) under each category is determined by the diagonal elements of the matrix. The row-wise summation of elements for each category other than the diagonal elements corresponds to the 'FN' of that category. The column-wise summation of elements for each category other than the diagonal element corresponds to the 'FP' of that category. Similarly, 'TN' of the specific category is determined by summing the elements of the matrix other than the elements in the corresponding row and column of the specic category.

For example, among the 73 Mild dysplasia testing images, 68 images have been successfully classified (TP) and the remaining 5 images (first row-wise summation) have been misclassified to any of the non-mild dysplasia categories (FN). Similarly 4 images (first column-wise summation) from the other three categories (non-mild dysplasia) have been misclassified as Mild dysplasia category (FP). In the Table 4, the classification accuracy of RBF in class 1 (Mild dysplasia) type tumor is 95.06%, class 2 (Moderate dysplasia) is 96.09%, class 3 (Severe dysplasia) is 95.037% and class 4 (carcinoma *in situ*) is 96.09%. The miss classification rate of class 1 (Mild dysplasia) and class 3 (Severe dysplasia) type tumor is high compared to the other two classes. The individual class and overall class accuracy calculation procedure are given in Eq. 12 and 13:

$$\text{Individual class accuracy for ith class} = \text{TP}(i)/\text{class}(i) \quad (12)$$

where, TP(i) is correctly classified instances of the class (i)

$$\text{Overall classification accuracy} = \left(\sum_i \text{TP}(i)/\sum_i \text{class}(i)\right)100 \quad (13)$$

In Table 5, the classification accuracy of SVM in class 1 type is 97.16%, class 2 is 97.51%, class 3 is 96.45%, class 4 is 97.51% and the overall classification accuracy is 94.32.

Table 2: Experimental image dataset for classification

Tumor type	Training data	Testing data	Total no of images
Mild dysplasia	40	73	113
Moderate dysplasia	40	65	105
Severe dysplasia	40	70	110
Carcinoma *in situ*	40	74	114

Table 3: Confusion matrix of proposed method

	Ground truth class (Assigned by radiologist)			
Class predicted	Mild dysplasia	Moderate dysplasia	Severe dysplasia	Carcinoma *in situ*
Mild dysplasia	68	1	2	2
Moderate dysplasia	1	61	2	1
Severe dysplasia	2	2	65	1
Carcinoma *in situ*	1	1	2	70
Individual class accuracy	98.58	99.29	97.87	97.97
Overall classification accuracy	96.80			

Table 4: Performance measure of RBF

Class predicted	TP	TN	FP	FN	Sensitivity (%)	Specificity (%)	Accuracy (%)
Mild dysplasia	65	203	6	8	89.04	97.12	95.03
Moderate dysplasia	60	211	6	5	92.30	97.23	96.09
Severe dysplasia	62	206	6	8	88.57	97.16	95.03
Carcinoma *in situ*	70	201	7	4	94.59	96.63	96.09
Overall classification accuracy	91.13						

Table 5: Performance measure of SVM

Class predicted	TP	TN	FP	FN	Sensitivity (%)	Specificity (%)	Accuracy (%)
Mild dysplasia	68	206	3	5	93.15	98.56	97.16
Moderate dysplasia	61	214	3	4	93.84	98.61	97.51
Severe dysplasia	65	207	5	5	92.85	97.64	96.45
Carcinoma *in situ*	72	203	5	2	97.29	97.59	97.51
Overall classification accuracy	94.32						

Table 6: Performance measure of Proposed method

Class predicted	TP	TN	FP	FN	Sensitivity (%)	Specificity (%)	Accuracy (%)
Mild dysplasia	70	208	1	3	95.89	99.52	98.58
Moderate dysplasia	63	217	0	2	96.92	100	99.29
Severe dysplasia	67	209	3	3	95.71	98.58	97.87
Carcinoma *in situ*	73	203	5	1	98.64	97.59	97.97
Overall classification accuracy	96.80						

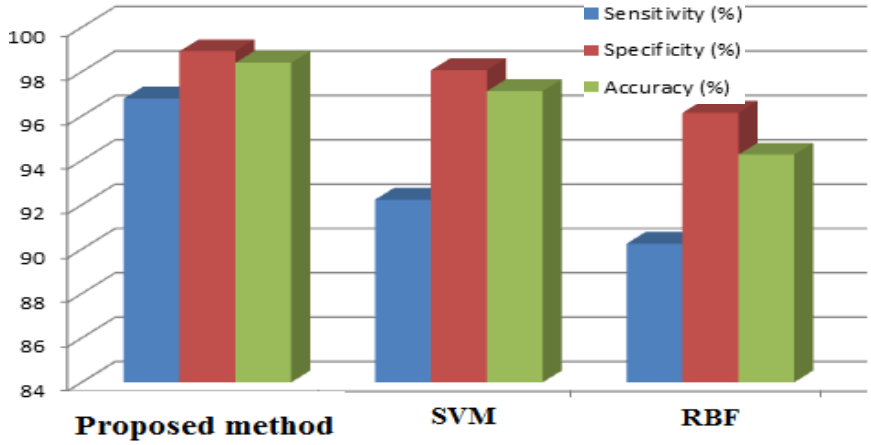

Fig. 3: The overall, experimental results of existing and proposed methods

The miss classification rate of class 1 and 3 types is high compared to the other two classes. In the Table 6, the classification accuracy of proposed method in class 1 type tumor is 98.58%, class 2 is 99.29%, class 3 is 97.87% and class 4 is 97.97%. For comparative analysis, the proposed cervical cancer classification system is compared to other neural network based methods such as RBF and SVM. The overall classification accuracy of the proposed method is 96.80%, SVM is 94.32% and RBF is 91.13%. The obtained results depict that the proposed multi class cancer classification approach produces better results compared to the other classifiers. The overall classification results of sensitivity, specificity and accuracy of existing and proposed method are shown in Fig. 3.

CONCLUSION

In this study, a novel cervical cancer classification system is developed which includes feature extraction and multiclass classification of four classes of cervical cancer types such as mild dysplasia, moderate dysplasia, severe dysplasia and carcinoma in situ. These cancer classes may have similar characteristics in their intensity and texture pattern; however, these cancer classes differ in their location, size and shape. The proposed method is developed by multi model-texture features and RBF kernel based support vector machine. The overall classification accuracy of the proposed method is 96.8% but the existing methods RBF and SVM produce 91.32 % and 94.32% respectively. The developed methods for feature extraction and classification of cervical cancer can be amalgamated to develop a CAD system. This system would be beneficial to radiologists for precise localization, diagnosis and interpretation of cervical cancer on PAP smear images.

REFERENCES

Chen, L., C.P. Chen and M. Lu, 2011. A multiple-kernel fuzzy C-means algorithm for image segmentation. IEEE. Trans. Syst. Man Cybern. Part B., 41: 1263-1274.

Cobzas, D., N. Birkbeck, M. Schmidt, M. Jagersand and A. Murtha, 2007. 3D variational brain tumor segmentation using a high dimensional feature set. Proceedings of the 2007 IEEE 11th International Conference on Computer Vision, October 14-21, 2007, IEEE, Rio de Janeiro, Brazil, ISBN: 978-1-4244-1631-8, pp: 1-8.

Daugman, J., 1988. Complete discrete 2-D Gabor transforms by neural networks for image analysis and compression. IEEE Trans. Acoust. Speech, Signal Process., 36: 1169-1179.

Demirkaya, O., 2002. Anisotropic diffusion filtering of PET attenuation data to improve emission images. Phys. Med. Biol., 47: N271-N278.

Jayachandran, A. and R. Dhanasekaran, 2013. Brain tumor detection using fuzzy support vector machine classification based on a texton co-occurrence matrix. J. Imaging Sci. Technol., 57: 10507-1-10507-7.

Julesz, B., 1981. Textons, the elements of texture perception and their interactions. Nat., 290: 91-97.

Khotanlou, H., O. Colliot, J. Atif and I. Bloch, 2009. 3D brain tumor segmentation in MRI using fuzzy classification, symmetry analysis and spatially constrained deformable models. Fuzzy Sets Syst., 160: 1457-1473.

Kiviat, N., 1996. Natural history of cervical neoplasia: Overview and update. Am. J. Obstetrics Gynecology, 175: 1099-1104.

Kurman, R.J., D.E. Henson, A.L. Herbst, K.L. Noller and M.H. Schiffman *et al*., 1994. Interim guidelines for management of abnormal cervical cytology. Jama, 271: 1866-1869.

Lin, J.S., K.S. Cheng and C.W. Mao, 1996. Segmentation of multispectral magnetic resonance image using penalized fuzzy competitive learning network. Comput. Biomed. Res., 29: 314-326.

Marinakis, Y., M. Marinaki and G. Dounias, 2008. Particle swarm optimization for pap-smear diagnosis. Expert Syst. Appl., 35: 1645-1656.

Mishra, R., 2010. MRI based brain tumor detection using wavelet packet feature and artificial neural networks. Proceedings of the International Conference and Workshop on Emerging Trends in Technology, February 26-27, 2010, ACM, Mumbai, India, ISBN: 978-1-60558-812-4, pp: 656-659.

Mukhopadhyay, S. and B. Chanda, 2003. Multiscale morphological segmentation of gray-scale images. IEEE. Trans. Image Process., 12: 533-549.

Mustafa, N., N.A. MatIsa, U.K. Ngah, M.Y. Mashor and K.Z. Zamli, 2004. Linear contrast enhancement processing on preselected cervical cell of Pap smear images. Technical J. Sch. Electr. Electron. Eng., 10: 30-34.

Peng, Y., M. Park, M. Xu, S. Luo and J.S. Jin et al., 2010. Detection of nuclei clusters from cervical cancer microscopic imagery using C4. Proceedings of the 2010 2nd International Conference on Computer Engineering and Technology (ICCET), April 16-18, 2010, IEEE, Chengdu, China, ISBN: 978-1-4244-6347-3, pp: V3-593-V3-597.

Pradhan, N. and A.K. Sinha, 2010. Development of a composite feature vector for the detection of pathological and healthy tissues in FLAIR MR images of brain. ICGST-BIME, J., 10: 1-11.

Shen, S., W. Sandham, M. Granat and A. Sterr, 2005. MRI fuzzy segmentation of brain tissue using neighborhood attraction with neural-network optimization. IEEE Trans. Inform. Technol. Biomed., 9: 459-467.

Yang, M.S.F., Y.K. Chan and Y.P. Chu, 2008. Edge enhancement nucleus and cytoplast contour detector of cervical smear images. IEEE. Trans. Syst. Man Cybern. Part B., 38: 353-366.